Proc. Indian Acad. Sci. (Math. Sci.), Vol. 92, No. 3, December 1983, pp. 143–155
© Printed in India.

Dusty effects on pulsating viscous flow of two immiscible fluids between two parallel plates

P K JHA* and M P PATERIYA

*Department of Physics
Department of Mathematics, Government College of Engineering and Technology, Raipur 492 002, India

MS received 8 September 1982; revised 23 May 1983

Abstract. The flow of two immiscible incompressible dusty viscous fluids between two parallel plates generated by a pulsating pressure gradient is investigated. Velocity fields for the fluid-particle system along with the expressions for the skin friction drag at the plates are obtained and studied graphically. It is found that there is an immediate response to pressure fluctuations in the first stream at low frequency range $0 < \sigma \leqslant 4$ being maximum at $\sigma = 4$. On the contrary, the second stream is more responsive to fluctuations at relatively higher frequencies. The maximum response in this case is shifted to $\sigma = 16$.

Keywords. Parallel plates; immiscible fluids; pulsatile flow; dusty effects; Stokes-Saffman layer.

1. Introduction

Problems on pulsating flows of fluids and problems associated with flows of immiscible fluids are of great theoretical and technical interest. Many authors like Phillips and Chiang [5], Bhattacharya and Nanda [1], Kant [3], Napolitano [4] and others have paid their attention to such flows. Recently, Gupta and Goyal [2] have studied the problem of pulsating flow of n-immiscible viscous fluids between two parallel plates. But they have not considered the effect of dust contamination on the flow although the presence of dust particles in the fluids can change the flow characteristics to a large extent.

In the present analysis, we have discussed dusty effects on the pulsatile flow of two immiscible viscous fluids between two parallel plates when the pressure gradient fluctuates about a steady mean. This study does not appear to have engaged the attention of researchers so far. Explicit expressions for the velocity fields of the fluid-particle system and skin friction at the plates have been derived and studied graphically for different density distributions and species of dust particles. It is observed that response to pressure gradient fluctuations is quicker in the first stream than in the second. Moreover, the magnitude of skin friction at the lower plate is much greater than that at the upper plate and its clean fluid value.

2. Governing equations

Consider unsteady motion of two viscous incompressible immiscible dusty fluids each occupying a height h between two stationary parallel flat plates kept at a distance $2h$

apart. Let μ_1, μ_2 and ρ_1, ρ_2 be respectively the coefficients of viscosity and densities of the fluids from lower to the upper plate. We choose a system of rectangular cartesian coordinates such that y' axis is perpendicular to the plates $y' = 0, y' = 2h$. The x' axis is chosen along the lower plate in the direction of pressure gradient. Let U_i' and V_i' be the velocities of the ith ($i = 1, 2$) fluid and dust therein respectively along x' axis, N_i the number density of dust particles, m_i and r_i be respectively the mass and radius of a single dust particle, p' the isotropic pressure, v_i ($= \mu_i/\rho_i$) the kinematic viscosity of the fluid, K_i ($= 6\pi\mu_i r_i$ for spherical particles) the Stokes coefficient of resistance, l_i ($= m_i N_i/\rho_i$) the mass concentration and τ_i ($= m_i/K_i$) the retardation time of dust particles in the ith fluid and t' the time. The plates are infinite in the x' and z' directions so that all the physical quantities are functions of y' and t' only. The dust particles are spherical and uniform in shape and size. The volume fraction of the solid particles is so small that the interaction between the solid particles is neglected. For the present problem, we have

$$U_i' = U_i'(y', t'),\ V_i' = V_i'(y', t'),\ N_i = N_{0i} = \text{constant}, \tag{1}$$

which satisfy the equation of continuity. Substituting (1) in equations of motion (Saffman [6]) and introducing the following dimensionless quantities

$$\left.\begin{aligned} &y = y'/h,\ U_i = hU_i'/v_i,\ V_i = hV_i'/v_i,\ t = v_i t'/h^2 \\ &Y_i = v_i\tau_i/h^2,\ k_i = \frac{h^2 K_i N_{0i}}{v_i\rho_i} = \frac{l_i}{Y_i}, f(t) = \frac{h^3}{v_i^2}\left(-\frac{1}{\rho_i}\frac{\partial p_i}{\partial x'}\right), \end{aligned}\right\} \tag{2}$$

we obtain the following equations of motion

$$\frac{\partial U_i}{\partial t} = f(t) + \frac{\partial^2 U_i}{\partial y^2} + k_i(V_i - U_i) \tag{3}$$

$$Y_i\frac{\partial V_i}{\partial t} = U_i - V_i. \tag{4}$$

Eliminating V_i between (3) and (4) we derive

$$Y_i\frac{\partial^2 U_i}{\partial t^2} + (1 + l_i)\frac{\partial U_i}{\partial t} = [f(t) + Y_i f'(t)] + \left[\frac{\partial^2 U_i}{\partial y^2} + Y_i\frac{\partial^3 U_i}{\partial t\,\partial y^2}\right], \tag{5}$$

where $f'(t) = \dfrac{\mathrm{d}f(t)}{\mathrm{d}t}$.

Equation (5) is to be solved under the following boundary conditions

$$\left.\begin{aligned} &U_1 = V_1 = 0 \text{ at } y = 0 \\ &U_2 = V_2 = 0 \text{ at } y = 2 \end{aligned}\right\}. \tag{6}$$

For uniform pulsating flow,

$$f(t) = x_{0i} + \mathrm{Re}\sum_{m=1}^{\infty} x_{mi}\exp(Jm\sigma t),\ J = \sqrt{-1}, \tag{7}$$

where Re denotes the real part. Coefficients x_{0i} and x_{mi} are Fourier constants of function $f(t)$. In view of (7) we take

$$U_i = U_0^{(i)} + \mathrm{Re}\sum_{m=1}^{\infty} U_m^{(i)}\exp(Jm\sigma t), \tag{8}$$

$$V_i = V_0^{(i)} + \mathrm{Re} \sum_{m=1}^{\infty} V_m^{(i)} \exp(Jm\sigma t), \tag{9}$$

where $U_0^{(i)}$, $V_0^{(i)}$, $U_m^{(i)}$, $V_m^{(i)}$ are functions of y only. Substituting (7) and (8) in (5) and comparing terms of the same family we get

$$(\mathrm{d}^2 U_0^{(i)}/\mathrm{d}y^2) + x_{0i} = 0, \tag{10}$$

$$(\mathrm{d}^2 U_m^{(i)}/\mathrm{d}y^2) - \lambda_i U_m^{(i)} + x_{mi} = 0, \tag{11}$$

where $$\lambda_i = \alpha_i + J\beta_i,\ \alpha_i = \frac{m^2 l_i Y_i \sigma^2}{1 + m^2\sigma^2 Y_i^2},\ \beta_i = \left[1 + \frac{l_i}{1 + m^2\sigma^2 Y_i^2}\right] m\sigma. \tag{12}$$

The conditions (6) are reduced to

$$\left.\begin{aligned} U_0^{(1)} = U_m^{(1)} = 0,\ V_0^{(1)} = V_m^{(1)} = 0 \text{ at } y = 0 \\ U_0^{(2)} = U_m^{(2)} = 0,\ V_0^{(2)} = V_m^{(2)} = 0 \text{ at } y = 2 \end{aligned}\right\}. \tag{13}$$

Neglecting surface tension at the interface and assuming that for moderate pulsation the shape of the interface will not change, the fluid velocities at the interface can be taken as

$$\frac{\nu_1}{h} U_i = A_1 + \mathrm{Re} \sum_{m=1}^{\infty} (Am)_1 \exp(Jm\sigma t) \text{ on } y = 1,\ i = 1, 2, \tag{14}$$

where A_1 and $(Am)_1$ are constants to be determined. Substituting (8) in (14) we derive

$$\frac{\nu_1}{h} U_0^{(1)} = \frac{\nu_2}{h} U_0^{(2)} = A_1 \text{ on } y = 1, \tag{15}$$

$$\frac{\nu_1}{h} U_m^{(1)} = \frac{\nu_2}{h} U_m^{(2)} = (Am)_1 \text{ on } y = 1. \tag{16}$$

3. Solution

3.1 *Steady part*

The solution of (10) is

$$U_0^{(i)} = -\tfrac{1}{2} x_{0i} y^2 + B_0^{(i)} y + C_0^{(i)},\ i = 1, 2, \tag{17}$$

which represents the parabolic flow for the steady part of the velocity distribution. Using (13), (15) and (17) we get

$$\left.\begin{aligned} B_0^{(1)} &= \frac{h}{\nu_1} A_1 + \tfrac{1}{2} x_{01},\ C_0^{(1)} = 0 \\ B_0^{(2)} &= -\frac{h}{\nu_2} A_1 + \tfrac{3}{2} x_{02},\ C_0^{(2)} = \frac{2h}{\nu_2} A_1 - x_{02} \end{aligned}\right\} \tag{18}$$

3.2 *Unsteady part*

Solving (11) we derive

$$U_m^{(i)} = B_i \cosh(\theta_i + J\phi_i) y + C_i \sinh(\theta_i + J\phi_i) y + \varepsilon_i,\ i = 1, 2, \tag{19}$$

where

$$\theta_i = \left[\frac{\alpha_i + (\alpha_i^2 + \beta_i^2)^{1/2}}{2}\right]^{1/2}, \quad \phi_i = \left[\frac{(\alpha_i^2 + \beta_i^2)^{1/2} - \alpha_i}{2}\right]^{1/2},$$

$$\varepsilon_i = \frac{x_{mi}(\alpha_i - J\beta_i)}{\alpha_i^2 + \beta_i^2}. \tag{20}$$

From (13), (16) and (19) B_i and C_i are evaluated as

$$B_1 = -\varepsilon_1, \; C_1 = \frac{(h/\nu_1)(Am)_1 + \varepsilon_1\{\cosh(\theta_1 + J\phi_1) - 1\}}{\sinh(\theta_1 + J\phi_1)},$$

$$B_2 = \frac{[\{(h/\nu_2)(Am)_1 - \varepsilon_2\}\sinh 2(\theta_2 + J\phi_2) + \varepsilon_2 \sinh(\theta_2 + J\phi_2)]}{\sinh(\theta_2 + J\phi_2)},$$

$$C_2 = \frac{[\{\varepsilon_2 - (h/\nu_2)(Am)_1\}\cosh 2(\theta_2 + J\phi_2) - \varepsilon_2 \cosh(\theta_2 + J\phi_2)]}{\sinh(\theta_2 + J\phi_2)}. \tag{21}$$

From (8), (17) and (19) the complete velocity distribution in the ith ($i = 1, 2$) fluid is obtained as

$$U_i = [U_i]_0 + \mathrm{Re}\sum_{m=1}^{\infty}\{B_i \cosh(\theta_i + J\phi_i)y + C_i \sinh(\theta_i + J\phi_i)y + \varepsilon_i\}\exp(Jm\sigma t). \tag{22}$$

Substituting (8) and (9) in (4), comparing terms and using (22) we get

$$V_i = [V_i]_0 + \mathrm{Re}\sum_{m=1}^{\infty}\left(\frac{1 - Jm\sigma Y_i}{1 + m^2\sigma^2 Y_i^2}\right)\{B_i \cosh(\theta_i + J\phi_i)y + C_i \sinh(\theta_i + J\phi_i)y + \varepsilon_i\}\exp(Jm\sigma t) \tag{23}$$

$$U_i - V_i = \mathrm{Re}\sum_{m=1}^{\infty}\left\{\frac{m\sigma Y_i(m\sigma Y_i + J)}{1 + m^2\sigma^2 Y_i^2}\right\}\{B_i \cosh(\theta_i + J\phi_i)y + C_i \sinh(\theta_i + J\phi_i)y + \varepsilon_i\}\exp(Jm\sigma t) \tag{24}$$

where

$$[U_i]_0 = [V_i]_0 = -\tfrac{1}{2}x_{0i}y^2 + B_0^{(i)}y + C_0^{(i)}. \tag{25}$$

From (25) it is seen that steady parts of the velocity functions are identical. From (22) and (23) it is evident that the amplitude of the unsteady part of the dust velocity is less, being reduced by a factor $1/(1 + m^2\sigma^2 Y_i^2)^{1/2}$ from that of fluid velocity.

4. Determination of interface velocities

We consider the continuity of shear at the interface. This gives

$$\left(g_{1,2}\frac{\partial U_1}{\partial y}\right)_{y=1} = \left(\frac{\partial U_2}{\partial y}\right)_{y=1} \tag{26}$$

where $g_{1,2} = (\mu_1/\mu_2)\cdot(\nu_1/\nu_2)$ is the non-dimensional parameter representing the interplay between the viscous and inertia forces of the fluids. Inserting (22) in (26), using

(18) and (21) and equating terms of same family we derive

$$h\left(\frac{1}{\nu_2}+\frac{g_{1,2}}{\nu_1}\right)A_1 = \tfrac{1}{2}(x_{02}+g_{1,2}x_{01}) \tag{27}$$

$$g_{1,2}(\theta_1+J\phi_1)\left\{\frac{h}{\nu_1}(Am)_1-\varepsilon_1\right\}\coth(\theta_1+J\phi_1)+(\theta_2+J\phi_2).$$
$$\times\left[\left\{\frac{h}{\nu_2}(Am)_1-\varepsilon_2\right\}\coth(\theta_2+J\phi_2)+\varepsilon_2\operatorname{cosech}(\theta_2+J\phi_2)\right]$$
$$= -g_{1,2}\varepsilon_1(\theta_1+J\phi_1)\operatorname{cosech}(\theta_1+J\phi_1). \tag{28}$$

These relations provide constants A_1 and $(Am)_1$ which determine the interface velocity.

5. Skin friction

The skin friction at the plates are

$$T_1 = \left[\frac{\partial U_1}{\partial y}\right]_{y=0} = [T_1]_0 + \mathrm{Re}\sum_{m=1}^{\infty}(\theta_1+J\phi_1)C_1\exp(Jm\sigma t) \tag{29}$$

$$T_2 = \left[\frac{\partial U_2}{\partial y}\right]_{y=2h} = [T_2]_0 + \mathrm{Re}\sum^{\infty}(\theta_2+J\phi_2)\{B_2\sinh(\theta_2+J\phi_2)$$
$$+C_2\cosh 2(\theta_2+J\phi_2)\}\exp(Jm\sigma t) \tag{30}$$

where $$[T_1]_0 = B_0^{(1)},\ [T_2]_0 = -2x_{02}+B_0^{(2)} \tag{31}$$

6. Mean sectional velocities

The sectional mean velocities $U^*_{iMV(t)}$, $V^*_{iMV(t)}$ of the fluid particle system (for $i = 1, 2$) are

$$U^*_{1MV(t)} = \int_0^1 U_1(y,t)\,dy$$
$$= [U^*_{1MV}]_0 + \mathrm{Re}\sum_{m=1}^{\infty}\left[\frac{1}{(\theta_1+J\phi_1)}\{B_1\sinh(\theta_1+J\phi_1)\right.$$
$$\left.+C_1(\cosh(\theta_1+J\phi_1)-1)\}+\varepsilon_1\right]\exp(Jm\sigma t) \tag{32}$$

$$V^*_{1MV(t)} = \int_0^1 V_1(y,t)\,dy$$
$$= [V^*_{1MV}]_0 + \mathrm{Re}\sum_{m=1}^{\infty}\left\{\frac{1-Jm\sigma Y_1}{1+m^2\sigma^2Y_1^2}\right\}$$
$$\times\left[\frac{1}{(\theta_1+J\phi_1)}\{B_1\sinh(\theta_1+J\phi_1)\right.$$
$$\left.+C_1(\cosh(\theta_1+J\phi_1)-1)\}+\varepsilon_1\right]\exp(Jm\sigma t), \tag{33}$$

$$U^*_{2MV(t)} = \int_1^2 U_2(y,t)\,dy$$
$$= [U^*_{2MV}]_0 + \mathrm{Re}\sum_{m=1}^{\infty}\left[\frac{2}{(\theta_2+J\phi_2)}\{B_2\cosh\tfrac{3}{2}(\theta_2+J\phi_2)\right.$$
$$\left.+C_2\sinh\tfrac{3}{2}(\theta_2+J\phi_2)\}\sinh\frac{(\theta_2+J\phi_2)}{2}+\varepsilon_2\right]\exp(Jm\sigma t) \tag{34}$$

$$V^*_{2MV(t)} = \int_1^2 V_2(y,t)\,dy$$

$$= [V^*_{2MV}]_0 + \mathrm{Re}\sum_{m=1}^{\infty}\left\{\frac{1-Jm\sigma Y_2}{1+m^2\sigma^2 Y_2^2}\right\}$$

$$\times\left[\frac{2}{\theta_2+J\phi_2}\left\{B_2\cosh\tfrac{3}{2}(\theta_2+J\phi_2)\right.\right.$$

$$\left.\left.+C_2\sinh\tfrac{3}{2}(\theta_2+J\phi_2)\right\}\sinh\frac{(\theta_2+J\phi_2)}{2}+\varepsilon_2\right]\exp(Jm\sigma t) \tag{35}$$

where

$$\left.\begin{aligned}[U^*_{1MV}]_0 &= [V^*_{1MV}]_0 = -\frac{x_{01}}{6}+\frac{B_0^{(1)}}{2}\\ [U^*_{2MV}]_0 &= [V^*_{2MV}]_0 = -\tfrac{7}{6}x_{02}+\tfrac{3}{2}B_0^{(2)}+C_0^{(2)}\end{aligned}\right\}. \tag{36}$$

7. Boundary layers

When θ_i and ϕ_i are large

$$\left.\begin{matrix}\cosh(\theta_i+J\phi_i)\\ \sinh(\theta_i+J\phi_i)\end{matrix}\right\} \simeq \tfrac{1}{2}\exp(\theta_i+J\phi_i),\ i=1,2. \tag{37}$$

Introducing the boundary layer coordinate

$\eta = 1-y$, on the interface,

$\eta = 2-y$, on the upper plate,

in (22)–(23) and taking real parts we get

$$U_i(y,t) = [U_i(y)]_0 + \sum_{m=1}^{\infty}\left[\frac{\exp(-\theta_i\eta)}{(\Sigma_i\theta_i^2+\Sigma_i\phi_i^2)^{1/2}}\{P_i\cos(\phi_i\eta-\psi-m\sigma t)\right.$$

$$\left.-Q_i\sin(\phi_i\eta-\psi-m\sigma t)\}+\{a_i\cos m\sigma t-b_i\sin m\sigma t\}\right] \tag{38}$$

$$V_i(y,t) = [V_i(y)]_0 + \sum_{m=1}^{\infty}\frac{1}{1+m^2\sigma^2Y_i^2}\left[\frac{(1+m^2\sigma^2Y_i^2)^{1/2}\exp(-\theta_i\eta)}{(\Sigma_i\theta_i^2+\Sigma_i\phi_i^2)^{1/2}}\right.$$

$$\times\{P_i\cos(\phi_i\eta-\psi_i-m\sigma t)-Q_i\sin(\phi_i\eta-\psi_i-m\sigma t)\}$$

$$\left.+\{L_i\cos m\sigma t+M_i\sin m\sigma t\}\right]. \tag{39}$$

Equations (38)–(39) show the existence of multiple boundary layers of thickness

$$\delta_i = \left\{\frac{\alpha_i+(\alpha_i^2+\beta_i^2)^{1/2}}{2}\right\}^{-1/2},\ i=1,2, \tag{40}$$

in the first and second dusty fluids respectively. These may be identified as the Stokes-Saffman layers and can be viewed either as a Classical Stokes layer modified by the presence of dust or as Saffman layer modified by pulsation. Outside the boundary

layers, in cores given by $\eta > \delta_i$, the exponential terms in (38)–(39) vanish and the velocity fields reduce to

$$U_i(y, t) = [U_i(y)]_0 + \sum_{m=1}^{\infty} [a_i \cos m\sigma t - b_i \sin m\sigma t], \; i = 1, 2$$

$$V_i(y, t) = [V_i(y)]_0 + \sum_{m=1}^{\infty} [L_i \cos m\sigma t + M_i \sin m\sigma t]. \tag{41}$$

7.1 *Saffman layer*

When mass concentration l_i of dust particles is very large and the size of dust particles are greater than a critical value ($Y_i > 1/m\sigma$), then $\alpha_i \gg \beta_i$. Hence, $\theta_i \simeq (\alpha_i)^{1/2}$, $\phi_i \simeq 0$ for $i = 1, 2$. Then from (22)–(23) we get

$$U_i(y, t) = [U_i(y)]_0 + \sum_{m=1}^{\infty} \left[\frac{\exp[-(\alpha_i)^{1/2}\eta]}{(\Sigma_i \alpha_i)} \{R_i \cos m\sigma t - S_i \sin m\sigma t\} + \right.$$

$$\left. + (a_i \cos m\sigma t - b_i \sin m\sigma t) \right], \tag{42}$$

$$V_i(y, t) = [V_i(y)]_0 + \sum_{m=1}^{\infty} \frac{1}{(1 + m^2\sigma^2 Y_i^2)^{1/2}} \left[\frac{(1 + m^2\sigma^2 Y_i^2)^{1/2}}{(\Sigma_i \alpha_i)} \times \right.$$

$$\times \exp[-(\alpha_i)^{1/2}\eta] \{R_i \cos(m\sigma t + x_i) + S_i \sin(m\sigma t + x_i)\} +$$

$$\left. + \{L_i \cos m\sigma t + M_i \sin m\sigma t\} \right]. \tag{43}$$

Equation (42)–(43) demonstrate the existence of thin boundary layers of thickness

$$p_i \simeq \frac{1}{(k_i)^{1/2}} \left(1 + \frac{1}{2m^2\sigma^2 Y_i^2}\right), \; i = 1, 2 \tag{44}$$

near the interface and the upper plate respectively. These may be identified as the modified (by the term $1/2m^2\sigma^2 Y_i^2$) Saffman layers. Thickness of these layers decreases with increase of m and σ. Boundary layers arising due to higher modes of pulsation ($m > 1$) are confined inside the boundary layer due to the fundamental mode ($m = 1$). Increasing values of number density or decreasing values of size of particles tend to decrease the boundary layer thickness.

7.2 *Stokes layers*

When frequency σ of pulsation is very large and mass concentration l_i of the particles is small, then $\beta_i \gg \alpha_i$. Hence from (20),

$$\theta_i \simeq c_i, \; \phi_i \simeq d_i$$

where

$$\left.\begin{aligned} c_i &= (m\sigma/2)^{1/2} \left[1 + \frac{k_i}{2m\sigma}\left(1 + \frac{1}{m\sigma Y_i}\right)\right], \; i = 1, 2 \\ d_i &= (m\sigma/2)^{1/2} \left[1 + \frac{k_i}{2m\sigma}\left(1 - \frac{1}{m\sigma Y_i}\right)\right] \end{aligned}\right\} \tag{45}$$

Hence from (22)–(23) we derive

$$U_i(y, t) = [U_i(y)]_0 + \sum_{m=1}^{\infty} \left[\frac{\exp(-c_i\eta)}{(\Sigma_i c_i^2 + \Sigma_i d_i^2)} \{F_i \cos(d_i\eta - \zeta - m\sigma t) - G_i \sin(d_i\eta - \zeta - m\sigma t)\} + \{a_i \cos m\sigma t - b_i \sin m\sigma t\} \right] \tag{46}$$

$$V_i(y, t) = [V_i(y)]_0 + \sum_{m=1}^{\infty} \frac{1}{1 + m^2\sigma^2 Y_i^2} \left[\frac{(1 + m^2\sigma^2 Y_i^2)^{1/2} \exp(-c_i\eta)}{\{\Sigma_i c_i^2 + \Sigma_i d_i^2\}^{1/2}} \times \{F_i \cos(d_i\eta - \xi_i - m\sigma t) - G_i \sin(d_i\eta - \xi_i - m\sigma t)\} + \{L_i \cos m\sigma t + M_i \sin m\sigma t\} \right] \tag{47}$$

Expressions (46)–(47) demonstrate the existence of boundary layers of thickness

$$q_i \simeq (2/m\sigma)^{1/2} \left[1 - \frac{k_i}{2m\sigma} \right], \; i = 1, 2 \tag{48}$$

near the interface and the upper plate respectively. These may be identified as the modified (by the term $k_i/2m\sigma$) Stokes layers. From (48) it is seen that the presence of dust particles decreases the thickness of the Stokes layers.

8. Flow under harmonic pressure gradient

We consider the particular case when the pressure gradient is given by

$$f(t) = x_{0i} + x_{ci} \cos \sigma t, \; i = 1, 2. \tag{49}$$

In this case, the sectional mean velocities and skin friction are obtained as

$$\left.\begin{aligned} U^*_{iMV(t)} &= [U^*_{iMV}]_0 + R_{iMV} \cos(\sigma t - \theta_{iMV}) \\ V^*_{iMV(t)} &= [V^*_{iMV}]_0 + R_{iD} \cos(\sigma t - \theta_{iD}), \; i = 1, 2, \\ T^*_i(t) &= [T^*_i]_0 + R_{iSF} \cos(\sigma t - \theta_{iSF}) \end{aligned}\right\} \tag{50}$$

where (R_{iMV}, θ_{iMV}), (R_{iD}, θ_{iD}) respectively denote the amplitude coefficients and phase lag of the sectional mean velocities from the wave of pressure gradient in the dusty fluids. Similarly, (R_{iSF}, θ_{iSF}) denote the corresponding quantities for the shear stresses at the plates in the direction of flow of the fluids.

The explicit forms of various coefficients in §§(7) and (8) are not given due to short of space.

9. Discussion

Figure 1 reveals that increasing values of the density distribution of particles amplify the response of the dusty mode in the first stream of low frequency range $0 < \sigma \leqslant 4$. The maximum response occurs at $\sigma = 4$ which is higher and sharper than that of the clean mode. This amplification is due to energy transfer from dust components to fluid particles at low frequencies and near the critical frequency. While light particles move

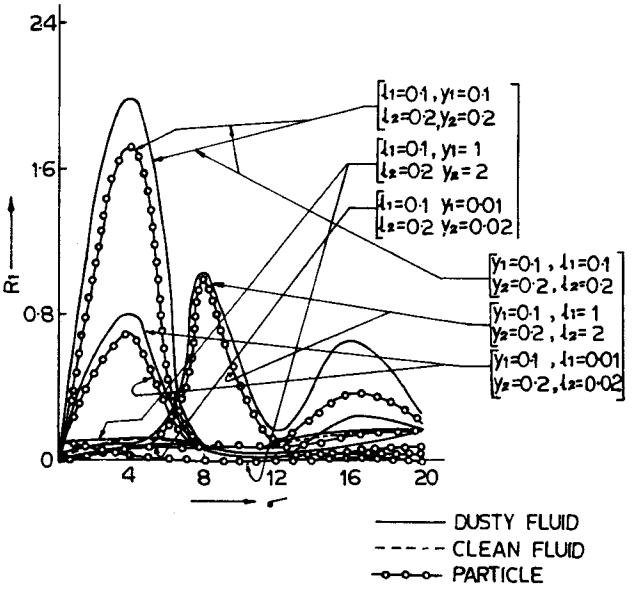

Figure 1. Variation of amplitude of sectional mean velocity of first dusty fluid with frequency.

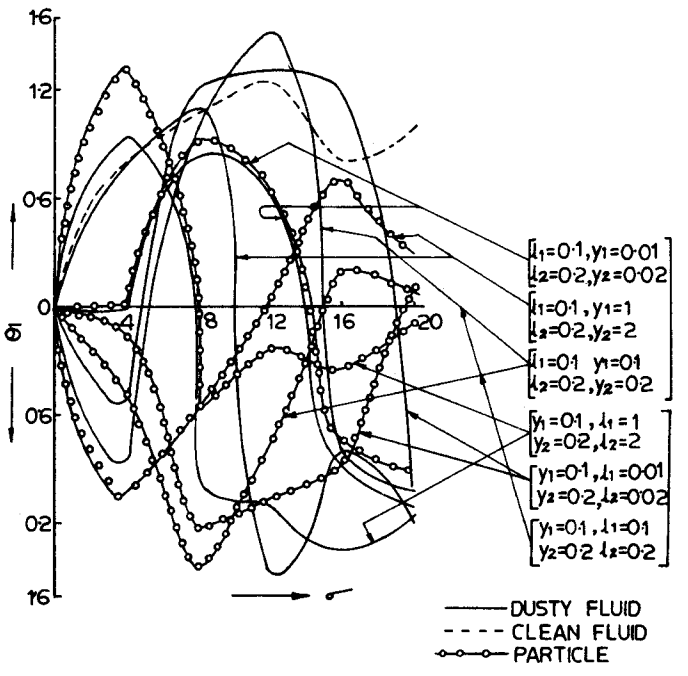

Figure 2. Variation of phase lag of sectional mean velocity in the first dusty fluid with frequency.

with the fluid, heavy particles show tendency towards sedimentation. Moreover, large density distribution or size of particles produces phase lag in the dusty mode in the first stream towards low frequencies while particles of low and moderate size or density distribution exert opposite influence (figure 2).

In the second stream (figure 3) there is almost no response to fluctuations at low frequencies. The maximum response occurs at $\sigma = 16$. As the density distribution of particles decreases, the response frequency increases and vice versa. Increasing values of the density of particle distribution enhance the phase lag of the dusty mode in this stream at low frequencies. Similar values of particle size display opposite behaviour (figure 4).

The amplitude of skin friction at the lower plate is much higher than at the upper plate and its clean fluid value (figure 5 and 6). While clean drag in both the streams always lags behind the pulsation, the dusty drag does so only partially (figures 7 and 8).

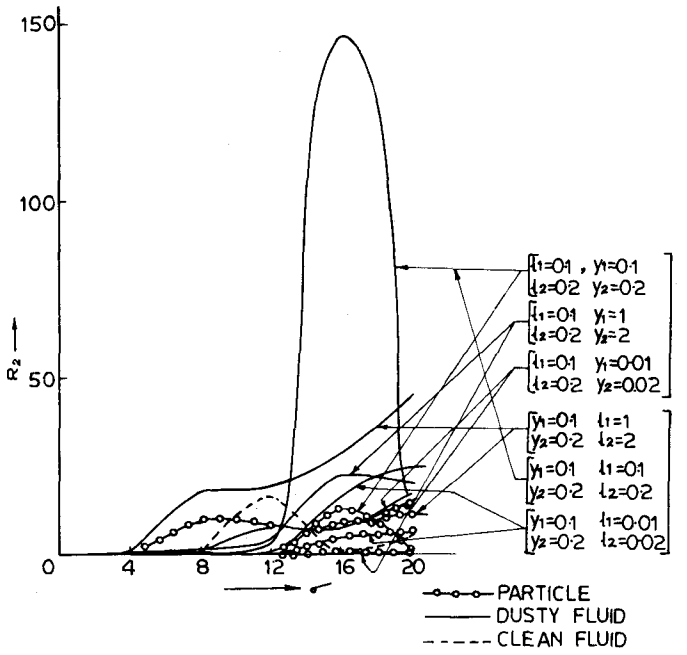

Figure 3. Variation of amplitude of sectional mean velocity of second dusty fluid with frequency.

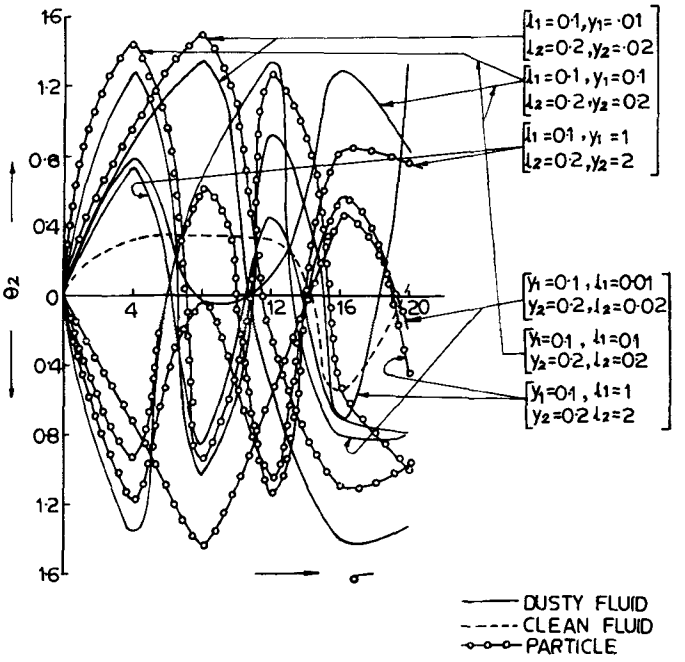

Figure 4. Variation of phase lag of sectional mean velocity in the second dusty fluid with frequency.

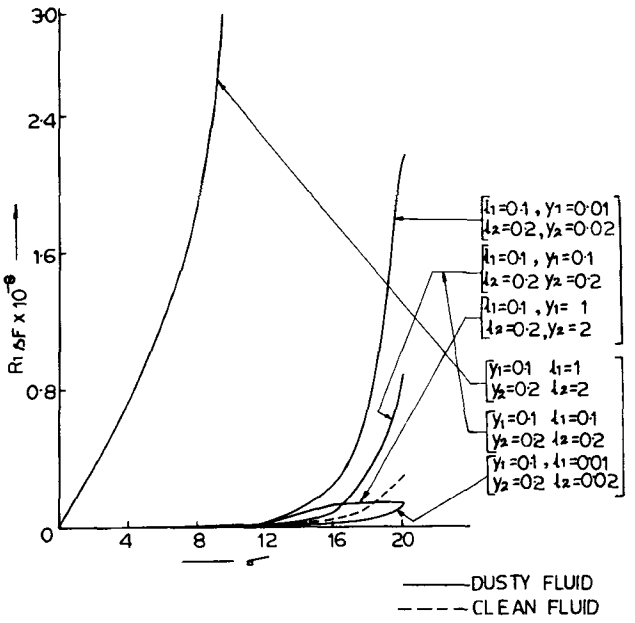

Figure 5. Variation of amplitude of skin friction at the lower plate with frequency.

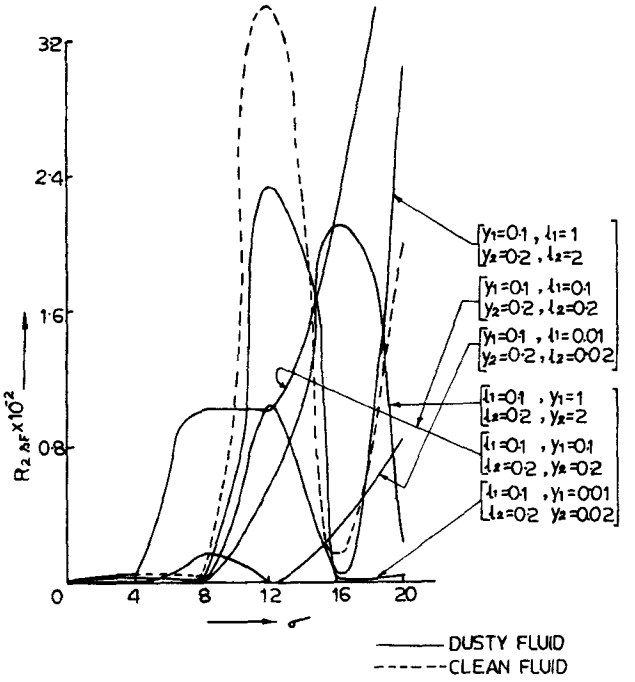

Figure 6. Variation of amplitude of skin friction at the upper plate with frequency.

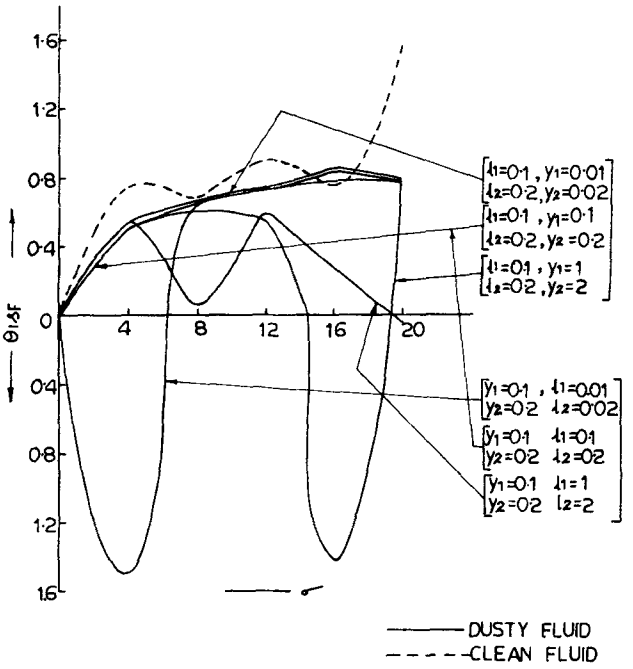

Figure 7. Variation of phase angle of skin friction at the lower plate with frequency.

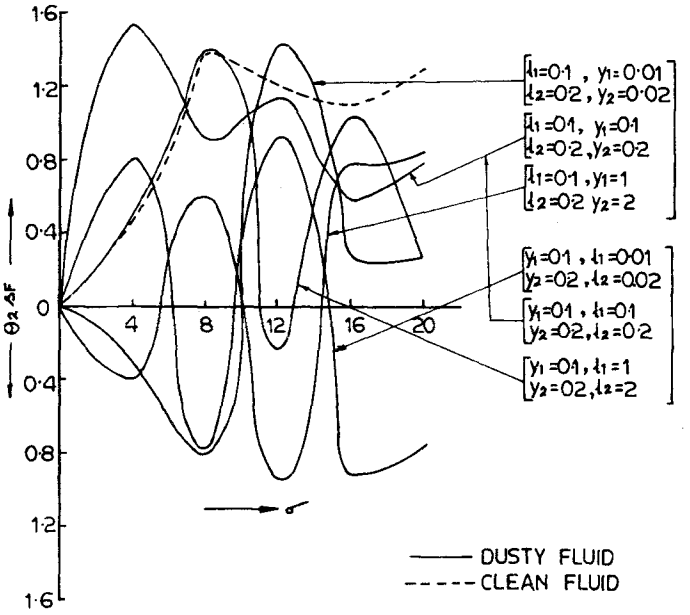

Figure 8. Variation of phase angle of skin friction at the upper plate with frequency.

Acknowledgements

The authors are grateful to the referee for his suggestions.

References

[1] Bhattacharya D K and Nanda R S 1979 *Proc. Indian Acad. Sci. (Math. Sci.)* **A88** 35
[2] Gupta M C and Goyal M C 1973 *Indian J. Pure Appl. Math.* **4** 680
[3] Kant R 1979 *Def. Sci. J. India* **29** 79
[4] Napolitano L G 1980 *Acta Astronaut.* **7** 461
[5] Phillips E M and Chiang S H 1973 *Int. J. Eng. Sci.* **11** 579
[6] Saffman P G 1962 *J. Fluid Mech.* **13** 120